JOURNAL OF SPACECRAFT AND ROCKETS
Vol. 32, No. 4, July–August 1995

Isotope and Parameter Effects in a Gas Core Nuclear Propulsion Reactor

John E. Tanner*
Westinghouse Idaho Nuclear Company, Idaho Falls, Idaho 83403

A combined radiation-transport, neutronic, and thermodynamic model of a gas-core nuclear propulsion reactor in steady-state operating conditions is presented. Arbitrary radial variation of composition and mass flow is provided for. The configurations asre constrained to a *k*-effective of unity. Local values of all variables are used at each mesh point, including recently evaluated opacities of uranium–hydrogen mixtures. Thrust and specific impulse are evaluated for several power levels (temperatures), engine sizes, reflector thicknesses, and flow and fuel–propellant mixing profiles, and for four fissile isotopes. Specific impulses and thrusts exceed those of a solid-core reactor at 3000 K even for the worst case of complete mixing of fuel and propellant.

Nomenclature

I_{sp}	= specific impulse, seconds
k	= opacity (Rosseland mean absorption coefficient)
k_{eff}	= neutron multiplication factor
Q_{abs}	= volume rate of energy absorption by flowing gases
Q_f	= volume rate of energy production by fission
R	= chamber radius
r	= radial location
r_1, T_1	= r, T at the wall surface
T	= temperature, K
σ	= Stefan–Boltzmann constant
∇	= vector differential operator
Δ	= annular thickness

Introduction

THE greatest uncertainty in the gas-core nuclear propulsion concept is the extent to which the fissile material can be hydrodynamically confined. This model was developed to show the effect on engine efficiency (specific impulse and thrust) of varying degrees of fuel confinement or lack thereof. Another purpose was to demonstrate the advantages of fissile isotopes besides ^{235}U.

Previous open-cycle models[1–4] have been essentially one-dimensional, have assumed sharp segregation of fuel and propellant (Kascak[4] allowed limited mixing), have combined only one or two of the important features (flow, radiation transport, neutronics, and thermodynamics), and have typically used regionally averaged rather than local properties for energy transport and balance calculations.

Recently Poston and Kammash[5,6] have constructed a thermal hydraulic model that is two-dimensional (except for the downflow boundary conditions), calculates laminar flow and diffusional mixing a priori, and uses local opacities and thermodynamic properties for radiation transport calculations. However, the model is not constrained by neutronic reactivity requirements.

The present work is a one-dimensional model that constrains the allowed configurations to $k_{eff} = 1 \pm 0.02$ and that uses neutronically calculated fission distributions as heat sources. Hydrodynamic flow patterns are not calculated a priori, but arbitrary mixing can be modeled, so that a full range of possibilities can be covered. Local values of opacity, fission energy production, composition, temperature, and enthalpy are used in the neutronics and radiation transport calculations. A total pressure of 1000 atm throughout is assumed. The effects of degree of propellant–fuel mixing, power level (average temperature), choice of fissile isotope, engine size, reflector thickness, and seeding on specific impulse and thrust are demonstrated.

Received March 9, 1994; revision received Aug. 1, 1994; accepted for publication Aug. 3, 1994.

*Fellow Scientist, Nuclear Engineering Department, ms 3428; currently at Lockheed Idaho Technologies Co., ms 3428, Box 1625, Idaho Falls, ID 83415.

Description

The plasma chamber was modeled in spherical symmetry. For the cases presented here, 20 spherical annuli (radial mesh points) were used. This model is compared in Fig. 1 with an idealized two-dimensional picture often discussed. Although the two-dimensional model (Fig. 1a) has a spherical shape and a spherical fuel region nearly concentric with the chamber wall, the fuel and hydrogen paths have only axial symmetry. Gas moves longitudinally down the chamber as well as from outside to inside, being heated along both parts of the path.

The present one-dimensional model (Fig. 1b) amounts to having fuel and propellant enter uniformly around the outer surface, and from there disperse in varying amounts to each of the annuli before being counted as having exited the chamber. Fission-generated heat radiates outward to warm the gases moving inward. Just as in the two-dimensional case, most of the gas exits before reaching the center.

The gases exiting from each annulus contribute an enthalpy and a mass flow rate according to an assigned velocity across the cross section of that annulus, and according to the density of an assigned composition at the calculated temperature. Mass flows and enthalpies are added (as if the annuli had emptied into a reservoir before exiting); then overall specific impulse and thrust are calculated. Complete conversion of enthalpy to macroscopic gas velocity in the throat and nozzle is assumed, i.e., the gas exits the nozzle in chemical equilibrium at a temperature near 0 K.

For calculating radiation transfer and k_{eff}, the compositions present in the chamber are used. That is, all gas present in a given annulus is counted, the portion on its way to an interior annulus as well as the portion on its way directly out the exit. Exit compositions versus compositions in transit (resident) are compared for two cases in Fig. 2.

Probably the biggest effect of this one-dimensional approximation is smearing the fuel out uniformly around each layer, rather than concentrating it in a path leading toward the center. Because the opacities of uranium and the transuranic elements are much higher than that of hydrogen, the opacity of most portions of the outer shells is higher than it would be in two-dimensional reality, thus allowing higher operating temperatures and thrust. However, the qualitative change in composition from center to outside is not changed. In a two-dimensional model the composition of most of the volume of a particular annulus would approximate what is here represented as an exit composition (a solid line in the examples of Fig. 2), whereas the rest of the annulus would have a much higher fuel fraction, so that the average for that annulus would correspond to what is here named a resident composition.

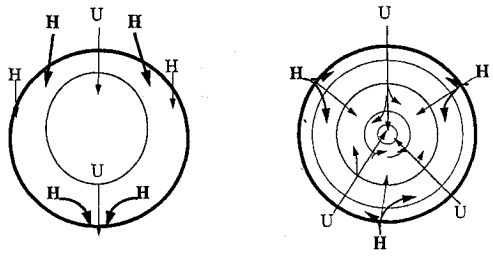

Fig. 1 Gas reactor chamber: a) as typically imagined in two dimensions and b) as modeled in one dimension.

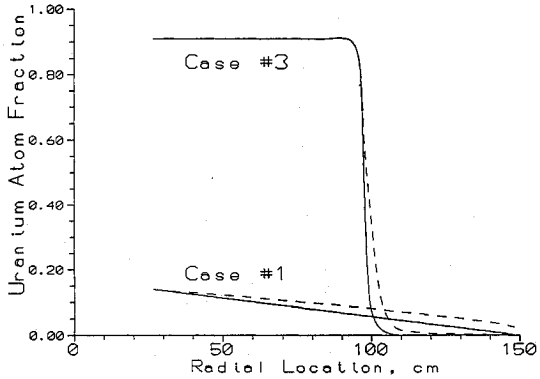

Fig. 2 Resident (dashed) and exit (solid) uranium atom fractions.

The reflector in most cases consisted of 5 cm of graphite at 3000 K, 40 cm of BeO at 2500 K, and 20 cm of BeO at 1200 K, in that order from the inside. In one case each, a 0.5-cm inner liner of tungsten or tungsten-184 at 3000 K was included.

Basic Relations

Since the plasma is optically dense (a blackbody), or nearly so at all but the lowest temperatures and uranium concentrations, a diffusion approximation of radiation transport may be used. The local radiation density is σT^4. Assuming a refractive index of unity, and ignoring scattering, the radiant heat flow through a region is[7] $-(4/3k)\nabla(\sigma T^4)$, and the radiation emanating from a local region is the divergence of this, or $-4/3\nabla\cdot(1/k)\nabla(\sigma T^4)$. The conservation equation for local energy balance is then

$$\text{radiant heat outflow} = \text{fission heat} - \text{heat to warm gas in transit}$$

$$-\frac{4}{3}\nabla\cdot\frac{1}{k}\nabla(\sigma T^4) = Q_f(r) - Q_{abs}(r) \tag{1}$$

In spherical symmetry, and with boundary conditions $dT/dr = 0$ at $r = 0$ and arbitrary wall temperature T_1, the solution is

$$\sigma T^4(r) = \sigma T_1^4 + \frac{3}{4}\int_r^{r_1}\frac{k(r')}{r'^2}\int_0^{r'} r''^2[Q_f(r'') - Q_{abs}(r'')]\,dr''\,dr' \tag{2}$$

For division into spherical annuli the above double integral was converted into a double sum. Within each annulus, k, Q_{abs}, and Q_f were taken as constant, but explicit functions of radius were integrated. The result is

$$\sigma T_j^4 = \sigma T_1^4 + \frac{1}{4}\sum_{m=j+1}^{n}\left[\frac{k_m\Delta_m}{r_m r_{m-1}}\sum_{i=1}^{m-1}(Q_f - Q_{abs})_i\left(r_i^3 - r_{i-1}^3\right)\right.$$

$$\left. + \frac{k_m}{2}\left(r_m^2 - 3r_{m-1}^2 + 2\frac{r_{m-1}^3}{r_m}\right)(Q_f - Q_{abs})_m\right] \tag{3}$$

In this equation subscripts for r and T refer to the outer boundaries of the respective annuli; n is the number of annuli, and equals 20 for all cases presented here. Although Q_f, Q_{abs}, and k are nominally functions of radius, they are actually functions of composition and temperature. Thus the solution to Eq. (3) is a temperature eigenvector.

Physical Data

Enthalpy, density, and opacity data for hydrogen over the required temperature and partial pressure ranges were obtained from Patch.[8,9] The corresponding data for uranium at pressures above 100 atm were obtained from Parks et al.[10] Uranium opacity data were extrapolated down to 1 atm by a procedure explained in Ref. 11. Uranium density data were extrapolated by assuming fixed ionization constants at each temperature. Enthalpies were assumed to vary linearly with uranium partial pressure.

Mixture properties were obtained by simple addition of the component properties at their respective partial pressures. However, component opacities were added only over short wavelength intervals, and the Rosseland sums for each composition and temperature were re-evaluated.[11] For most of the calculations a lower opacity limit of 5 cm^{-1} was imposed. This affected only the lower third of the temperature range for uranium partial pressures below 10 atm, and had a significant effect for only five of the cases. The values of the opacities and thermodynamic parameters calculated for uranium–hydrogen mixtures were also used for the mixtures with ^{239}Pu and $^{242}Am^m$ for lack of actual data for these two isotopes.

Fissile-isotope continuous-energy neutron cross sections were obtained by broadening the resonance peaks of the ENDF/B-V data with the NJOY[12] code for seven temperatures between 3000 and 50,000 K. The cross-section set at the next lower temperature than the region involved was used for the neutronics calculations. A cross-section set was prepared similarly for natural tungsten at 3000 K. Standard, continuous-energy MCNP[13] cross-section sets with unbroadened resonances were used for hydrogen, beryllium, oxygen, and tungsten-184.

Calculational Procedure

Table 1 distinguishes the arbitrarily adjustable parameters from those to be solved for. The functional forms of the variation of exit velocity and composition with radius were specified arbitrarily. Examples of velocities are given in Fig. 3. A composition magnitude parameter was adjusted to give $k_{eff} = 1 \pm 0.02$. Similarly, a velocity magnitude parameter was adjusted so that the energy adsorbed by the gases equaled the energy transported at the assumed temperatures, as indicated by a rough overall balance of input and output temperatures. Figure 4 is a flow chart of the steps involved.

Counting the outer boundaries, two temperature parameters could be specified, and the other $n - 1$ temperatures had to be solved for. The wall temperature was set at 3000 K, and for all cases except 3 and 3a, the volume average temperature was specified. For these latter cases, it was preferable to specify the center temperature.

Since for simplicity it was assumed that the gas is optically dense out to the wall, the only direct energy transfer from within the gas to the wall would be by gamma rays and fast neutrons, which were assumed to account for 7% of the total fission energy. Annular fission energies from the neutronics calculations were therefore normalized so that their sum over all annuli equaled 93% of the sum of gaseous enthalpy changes from 0 K up to the point of exit. Thus the fission energy assigned to the chamber exceeded the energy absorbed by the gases within the chamber by an amount that, as a boundary condition, was transferred to the wall. This plus the 7% of direct transfer equaled the energy needed to warm these gases to the assigned temperature of the wall surface just as they reached it from somewhere within the wall. Heat transfer within the wall was not modeled.

Table 1 Variables for n Layers

Quantity	Number of variables: Independent	Number of variables: Dependent	Requirement
Velocity	$n-1$	1	T (input range) = T (output range)
Composition	$n-1$	1	$k_{eff} = 1 \pm 0.02$
Temperature	1 or 2	$n-1$	T_i(input) = T_i(output), all i

Uranium-235 was chosen for the reference case because it is the fissile isotope most commonly discussed, even though it would give the poorest performance. The linear increase in velocity from center to outside and linear decrease of fuel atom fraction in that direction are a compromise between the goal of strict fuel–propellant segregation with no loss of propellant and the worst case of complete mixing. It also seems realistic.

A reflector optimized for weight as well as fuel efficiency would probably be thinner than used here. Calculations with a simpler system show that 60 cm of BeO at these temperatures is nearly full reflection.

A model of complete segregation of fuel and propellant would violate the assumption of optically dense propellant region, and require a different mathematical treatment. Since realistically at least a little mixing will take place, a small amount of fuel was allowed to "seed" the propellant in case 3. See Fig. 2.

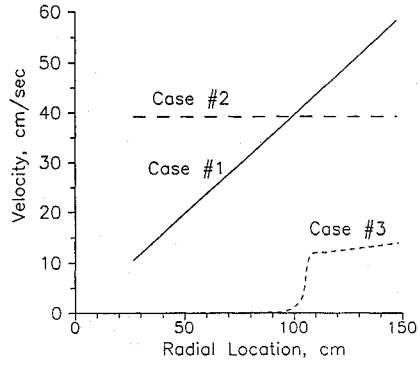

Fig. 3 Functional forms of gas velocities used.

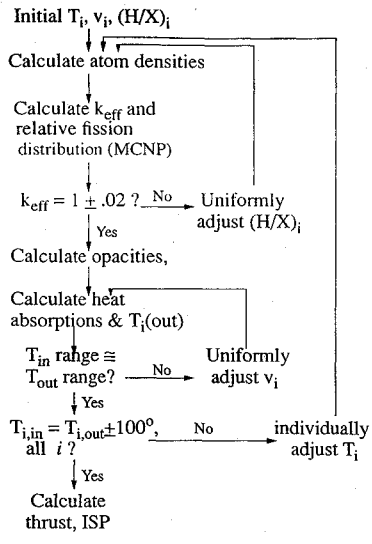

Fig. 4 Calculation flowchart.

Performance

Calculated thrust, I_{sp}, and fuel loss (H/fissile atom ratios in exit) for 18 cases are presented in Table 2. Cases 1–10 are for the highest power level (average temperature); cases 11 and 12, for an intermediate power level; and cases 13–15, for the lowest power level. Fuel and propellant residence times and fuel burnup fractions are also presented. Power level is not tabulated, but may be calculated in watts as $4.9 \times I_{sp}$ (s) × thrust (N). Values range from 75 MW for case 13 to 10 GW for case 9.

A solid-core nuclear fission reactor exhausting pure hydrogen at 3000 K would have an I_{sp} of 1010 s, with the hydrogen thermodynamic data and the ideal nozzle assumption used in the gas core calculations. The I_{sp} for all of the gas-core cases calculated here exceeds this, even in the extreme case of complete mixing. The high chamber temperatures assumed possible have more than compensated for the high atomic weight of the fuel assumed lost in the exhaust. A recalculation of case 1 for frozen hydrogen equilibrium in the throat and nozzle yielded only a small decrease in performance—2080-s I_{sp} and 129-kN thrust.

Comparing cases 1, 11, and 13, or cases 6 and 14, or cases 8 and 15, the thrust is approximately proportional to the 2.7th power of average temperature. Thrust requires transport of energy from the center outward. The decrease from a 4th-power law may be caused by higher opacities in the higher-temperature cases, which were a consequence of the higher fissile fractions required for criticality.

On progressing from nearly complete segregation of fuel and propellant to partial mixing and then to complete mixing (cases 3, 1, and 2, respectively), the thrust, and of course the fuel loss, increase. Heat generation becomes more uniform in this sequence, so that there is less dependence on radiation transport. The decrease in I_{sp} is probably caused by the increased fissile fraction in the exhaust.

^{239}Pu and ^{233}U give much better performance than ^{235}U, as expected, and are roughly equivalent. A close comparison between these two isotopes would require appropriate thermodynamic and opacity data for the ^{239}Pu calculations. The best performance is for $^{242}Am^m$. Seeding would be more important for this isotope because of the lower concentrations of heavy atoms to absorb radiation in the outer regions of the chamber.

Table 2 Specific impulse, thrust, fuel loss, average residence times, and burnup for various flow patterns, mixing ratios, temperatures, and isotopes

Case	Conditions different from reference case	I_{sp}, s	Thrust, kN	H/X at exit	Residence time, s		Burnup fraction
					Fissile	Hydrogen	
1	—[a]	2230	138.	39.7	9.9	4.8	3.4 – 6
2	Constant ^{235}U fraction and velocity everywhere	1770	165.	17.7	5.8	5.8	2.0 – 6
3	Nearly segregated core; reflector 5, 15.1, 10 cm	2250	20.9	771.	611.	21.	1.3 – 5
3a	Like case 3, but no seeding	1980	24.2	916.	534.	21.	1.1 – 5
4	Reflector 5, 20, 10 cm	1710	103.	20.	17.	8.2	1.9 – 6
5	Engine radius 2.00 m	2510	211.	55.	14.	6.7	4.5 – 6
6	^{233}U	3600	242.	214.	3.5	1.7	1.5 – 5
6a	^{233}U; no seeding	3570	251.	228.	3.4	1.6	1.5 – 5
7	^{233}U; 0.5 cm ^{184}W replaces 0.5 cm of graphite	3040	188.	107.	5.4	2.6	7.9 – 6
8	^{239}Pu	3300	245.	147.	3.8	1.8	1.0 – 5
9	$^{242}Am^m$	4330	474.	2106.	1.5	.7	1.1 – 4
10	$^{242}Am^m$; reflector 5, 20, 10 cm	4370	423.	1129.	1.7	.8	6.5 – 5
11	Center ≈36,400 K, average 22,479 K, wall 3000 K	2150	37.7	84.	38.	19.	3.7 – 6
12	Like case 11, but ^{233}U; 0.5 cm W (natural) in reflector	1220	25.0	17.2	245.	116.	9.3 – 7
13	Center ≈ 23,300 K, average 13,144 K, wall 3000 K	1880	8.2	233.	194.	94.	4.1 – 6
14	Like case 13, but ^{233}U	2330	16.0	878.	78.	38.	1.5 – 5
14a	Like case 14, but no seeding	2170	24.5	1009.	55.	27.	1.5 – 5
15	Like case 13, but ^{239}Pu	2330	19.0	751.	65.	32.	1.3 – 5

[a]Reference case: Linear radial dependence of ^{235}U atom fraction—zero at the wall. Linear radial increase of velocity from zero at the center. Cavity radius 1.50 m. Temperatures, center, ≈48,000 K; average, 32,036 K; wall, 3000 K. Reflector, 5 cm graphite at 3000 K, 40 cm BeO at 2500 K, 20 cm BeO at 1200 K. Seeded to opacity >5 cm^{-1}.

Note that an increase in engine size increases I_{sp} as well as thrust. A large core allows criticality to be achieved with a lower fuel fraction.

The use of a 0.5-cm liner of natural tungsten to protect the reflector (case 12) produced an unacceptable loss in performance. A brief calculation showed that TaC would have been a little worse. Isotopically separated ^{184}W may be acceptable (case 7) if needed to protect the reflector from hydrogen. Of course, if the liner were only needed near the throat, its effect would be much smaller than calculated here.

Burnup fractions were most strongly influenced by factors affecting the fuel fraction required for criticality, especially choice of isotope, but also engine radius and reflector thickness. However, temperature had relatively little effect on burnup, because the change in residence time was mostly canceled by the change in power, and hence fission rate. The generally low burnups are consistent with the short residence times.

Cases 3, 6, and 14 were recalculated (cases 3a, 6a, and 14a) with opacities not adjusted for the assumed seeding. These cases represent low to intermediate heavy-atom concentrations in the outer region. The direct effect was to decrease radiation absorption in the outer region of the chamber. In compensation the energy-balance calculation decreased temperatures and hence increased the second temperature derivative in this region to maintain absorption. This increased densities and mass ejection in all cases, and increased thrust. This density increase was the only significant factor for case 3, where center temperature was kept constant. In cases 6 and 14, where average temperatures were fixed, the code calculated an increase in overall energy output, which further increased thrust compared to the corresponding seeded cases.

Other Results

Sample temperature profiles are presented in Fig. 5. The flatness near the center and steep decrease near the wall have been found in previous nonhydrodynamic models, and are a consequence of the dependence of radiation transport on T^4, somewhat modified by the variation of the opacity with temperature and composition. Local net energy production for the same examples is shown in Fig. 6. Additional calculated results for case 1 are presented in Table 3.

Table 3 Details of the reference case

	Overall compositions		
	Fuel atomic fraction	Fuel weight fraction	Density, g/cm^3
Chamber	0.049	0.92	0.0411
Exhaust	0.025	0.85	
	Opacity		
	Nearly constant at $\approx$80 cm^{-1} at the center, increasing to $\approx$200 cm^{-1} near the wall		

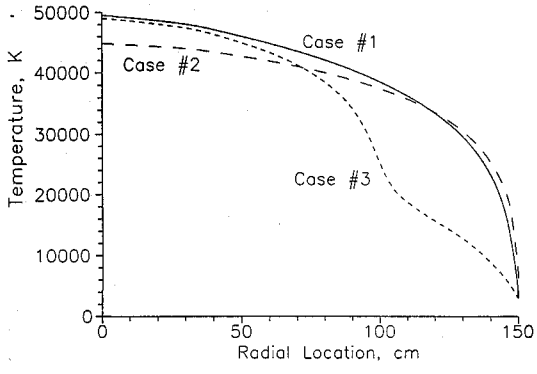

Fig. 5 Solved temperature profiles.

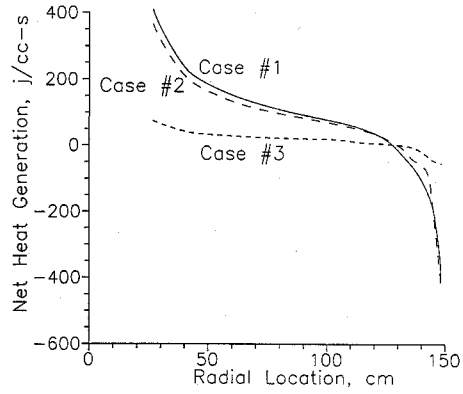

Fig. 6 Net energy production $Q(r)$.

Conclusions

It has been possible to remove many of the simplifying assumptions and restrictions previously used in one-dimensional gas-core nuclear propulsion reactor models.[1,2,4] Calculations indicate attractive specific impulses and thrusts, even if high fuel losses occur. The fuel cost and the problem of keeping it subcritical in storage would still be unattractive features.

Acknowledgment

This work was funded by the DOE-ID Laboratory Directed Research and Development program through Westinghouse Idaho Nuclear Co.

References

[1]Schnitzler, B. G., "Gas Core Reactors for Direct Nuclear Propulsion," EG&G Idaho Co., EGG-NE-9087, Idaho Falls, ID, June 1990.

[2]Bennett, R. G., "Gas Core Reactor Conceptual Development Task, Letter Rept.," EG&G Idaho Co., EGG-NE-10391, Idaho Falls, ID, Sept. 1991.

[3]Miles, V. A., and Kunze, J. F., "Stability Study of Co-Axial Gas Core Nuclear Rocket," Paper CONF-900109, *Proceedings of the 7th Symposium on Space Nuclear Power Systems*, American Inst. of Physics, 1990, pp. 71–76.

[4]Kascak, A. F., "Estimates of Local and Average Fuel Temperatures in a Gaseous Nuclear Rocket Engine," NASA-TN-D-4164, Sept. 1967.

[5]Poston, D. I., and Kammash, T., "A Comprehensive Thermal–Hydraulic Model of an Open-Cycle Gas Core Nuclear Rocket," Paper CONF-940101, *Proceedings of the 11th Symposium on Space Nuclear Power Systems*, American Inst. of Physics, 1994, pp. 473–479.

[6]Poston, D. I., and Kammash, T., "Hydrodynamic Fuel Containment in an Open-Cycle Gas Core Nuclear Rocket," Paper CONF-940101, *Proceedings of the 11th Symposium on Space Nuclear Power Systems*, American Inst. of Physics, 1994, pp. 1415–1420.

[7]Deissler, R. G., "Diffusion Approximation for Thermal Radiation in Gases with Jump Boundary Condition," *Journal of Heat Transfer*, Vol. 86, No. 2, 1964, pp. 240–246, Eq. (15).

[8]Patch, R. W., "Interim Absorption Coefficients and Opacities for Hydrogen Plasma at High Pressure," NASA TMX-1902, Oct. 1969.

[9]Patch, R. W., "Thermodynamic Properties and Theoretical Rocket Performance of Hydrogen to 100000 K and 1.01325 $\times$ 10^8 N/m^2," NASA SP-3069 and N72-12776, 1971.

[10]Parks, D. E., Lane, G., Stewart, J. C., and Peyton, S., "Optical Constants of Uranium Plasma," NASA CR-72348, GA-8244, Feb. 1968.

[11]Tanner, J. E., "Opacities of Uranium–Hydrogen Gas Mixtures at High Temperatures and Pressures," *Transactions of the American Nuclear Society*, Vol. 68, Part A, 1993, pp. 346–348.

[12]Anon., "NJOY91.13, A Code System for Producing Pointwise and Multigroup Neutron and Photon Cross Sections from ENDF/B Evaluated Nuclear Data," contributed by Los Alamos National Lab., PSR-171, RSIC, 1991.

[13]Anon., "MCNP 4-Monte Carlo Neutron and Photon Transport Code System," contributed by Los Alamos National Lab., RSIC Computer Code Collection, CCC-200A/B, version 4.2, Oak Ridge National Lab.

I. D. Boyd
Associate Editor